

THE COTTON-MOUTON EFFECT IN TERBIUM IRON GARNET

R. V. PISAREV, I. G. SINII, and G. A. SMOLENSKII

Institute of Semiconductors, U.S.S.R. Academy of Sciences

Submitted March 5, 1969

Zh. Eksp. Teor. Fiz. 57, 737-748 (September, 1969)

Mechanisms of magnetic birefringence of light in magnetically ordered crystals are considered. It is shown that birefringence of light moving perpendicular to the magnetization may arise as a result of the Cotton-Mouton effect (CME) and magnetostriction. The main isotropic contribution to the CME is ascribed to the exchange interaction between paramagnetic ions in various sublattices. Along with this there should exist in crystals a contribution to the CME due to the anisotropy of a single paramagnetic ion and also to anisotropic exchange interaction. These two contributions should lead to anisotropy of the CME which should be large in rare-earth garnets.

Magneto-optic birefringence was investigated in the terbium iron garnet $Tb_3Fe_5O_{12}$ at a wavelength of $\lambda = 1.15 \mu$, at temperatures between 77 and 295°K and in magnetic fields up to 23 kOe. At $T = 295^\circ K$ $\Delta n^{[100]} = 6 \times 10^{-5}$; with decreasing temperature birefringence increases and at 77°K $\Delta n^{[100]} = 70 \times 10^{-5}$. At 295°K $\Delta n^{[111]} = 3 \times 10^{-5}$; with decreasing temperature Δn changes sign at 200°K and at 77°K $\Delta n^{[111]} = -72 \times 10^{-5}$. Above the magnetic compensation point $T_C = 249^\circ K$ an increase of the external field H results in a decrease and below T_C to an increase of magnetic birefringence. An analysis of the $\Delta n(H, T)$ curves reveals that birefringence in $Tb_3Fe_5O_{12}$ is related to the CME as well as to magnetostriction. At the magnetic compensation point T_C a birefringence anomaly is observed which manifests itself in a double change of sign of the effect and an increase of the depolarization and of the scattering of light traversing the crystal. These phenomena are only observed in sufficiently strong magnetic fields and are a result of a forced phase transition from one ferromagnetic state to an antiferromagnetic one and then to another ferromagnetic state when the temperature is varied. Inversion of the magnetic sublattices at T_C results in a change of sign of Δn , whereas fluctuations of the direction and magnitude of the magnetic moments give rise to an increase in the depolarization and scattering of light.

1. INTRODUCTION

A NEW exchange-dipole mechanism of quadratic magneto-optical effects in ferro- and antiferromagnets has recently been proposed.^[1] This mechanism leads to unusually high values of the Cotton-Mouton effect (CME) in magnetic crystals below T_C , N . It can lead to the same order of magnitude of the magneto-optic effects quadratic in the magnetization, for example the CME, as the linear effects, for example the Faraday effect (FE). Large values of the CME $\Delta n_{C-M} \sim 10^{-3} - 10^{-5}$ have been observed experimentally in crystals with various structures: in ferromagnets with the garnet structure $Y_3Fe_5O_{12}$ and $Tb_3Fe_5O_{12}$,^[2] in the ferromagnet $RbNiF_3$,^[1] in the antiferromagnet with a weak moment $RbFeF_3$,^[1, 3, 4] in antiferromagnetic hematite $\alpha-Fe_2O_3$ ^[2] and in the ferromagnet $EuSe$.^[5] So far the majority of the magneto-optic investigations of ferro- and antiferromagnetic dielectrics was devoted to the FE which is linear in the magnetization. However, the large CME in magnetically ordered crystals and the comparative simplicity of observing the CME open up interesting possibilities of investigating exchange interactions in crystals, the temperature dependence of the sublattice magnetizations, the orientation of the magnetic moments with respect to the crystallographic axes, and other phenomena.

We note that the CME can be equally well used to investigate ferro- and antiferromagnets, whereas the lin-

ear magneto-optic effects can be used mainly to investigate ferromagnets.

Of great interest are, apparently, complex investigations of linear and quadratic effects which make it possible to study the spectral and temperature behavior of the dielectric permittivity and the magnetic permeability tensors of crystals and to elucidate the contribution of various interactions to these properties.

This paper is devoted to an investigation of the temperature and field dependences of the magnetic birefringence in terbium iron garnet (TbIG) as well as of the properties of the interaction of light with the crystal at the magnetic compensation point (T_C).

2. METHODOLOGICAL REMARKS

The magnetic birefringence and the depolarization and scattering of light near the magnetic compensation point was measured on a setup schematically illustrated in Fig. 1. The light from a helium-neon laser with a

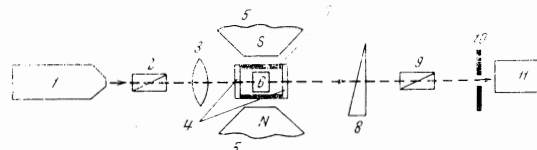


FIG. 1. Optical diagram of the experiment: 1 - helium-neon laser, 2 - polarizer, 3 - long-focus lens, 4 - cryostat windows, 5 - poles of the electromagnet, 6 - investigated crystal, 7 - cryostat, 8 - Berek compensator, 9 - analyzer, 10 - aperture (used in the light scattering experiments), 11 - photomultiplier.

power ~ 10 MW ($\lambda = 1.15 \mu$ passed through a polarizer and a focusing lens onto a crystal mounted in a cryostat with a controllable temperature. The cryostat was placed in the gap of an electromagnet with the magnetic field perpendicular to the direction of propagation of the light; the maximum field amounted to 23 kOe. The phase difference which the light acquired in the crystal was measured by means of an optical Berek compensator^[6] placed between a crossed polarizer and analyzer. Following the analyzer the light was incident on the cathode of a FEU-28 photomultiplier. The light was modulated with a frequency of 1500 cps and the signal was registered by means of a narrow-band amplifier and synchronous detector.

Magnetic birefringence occurs in a crystal as a result of the fact that two light waves polarized with $\mathbf{E} \parallel \mathbf{H}$ and $\mathbf{E} \perp \mathbf{H}$, where \mathbf{E} is the electric vector of the light wave and \mathbf{H} is the external magnetic field, propagating in the crystal perpendicular to the magnetization have different phase velocities. Plane-polarized light whose electric vector was oriented at an angle of 45° to the direction of the external magnetic field was incident on the crystal during the magnetic birefringence measurements. The components of \mathbf{E} parallel and perpendicular to the external field are then equal in amplitude and the birefringence is only connected with the difference in the phase velocities of these components. The relationship between the phase difference β and the difference between the refractive indices $\Delta n = n_{\parallel} - n_{\perp}$ is given by the formula

$$\beta = \frac{2\pi}{\lambda} \Delta n, \quad (1)$$

where λ is the wavelength of the light. Strong depolarization of the light transmitted through the crystal was observed in investigating the magnetic birefringence in the region of T_C , as well as in low magnetic fields. The experimental graphs show the fraction of the total light intensity with an undetermined phase difference.

We have also investigated the changes in the intensity of the light transmitted through the crystal in the region of T_C . In this experiment the compensator and analyzer were removed and after passing through the crystal the light was incident on the cathode of a photomultiplier placed at a distance of about 1 mm from the crystal. An aperture with a diameter ~ 3 mm was placed before the cathode. Only light which propagates through the crystal strictly along a straight line is recorded under these conditions, and it is obvious that the observed intensity variations of the signal in the region of T_C can be related to light scattering.

In this work we have investigated a 0.275-cm thick platelet of TbIG cut parallel to the (110) planes.

3. THE MAGNETIC PROPERTIES OF TERBIUM IRON GARNET

The crystal structure of garnet is described by the cubic space group $O_h^{10} - Ia3d$.^[7] The magnetic structure of rare-earth iron garnets^[8,9] can be imagined to consist of three nonequivalent sublattices: 1) the sublattice of Fe^{3+} iron ions in tetrahedral surroundings consisting of oxygen O^{2-} ions (crystallographic positions 24d), 2) Fe^{3+} ion sublattices in octahedral surroundings of O^{2-}

ions (16a positions), and 3) sublattices of yttrium or rare-earth ions (24c positions). The tetrahedral and octahedral sublattices are coupled by a strong negative exchange interaction which determines the Curie temperature of the garnets ($T_C = 568^\circ K$ for TbIG). The rare-earth sublattice is oriented antiparallel to the resulting magnetization of the two iron sublattices. In TbIG the magnetization of the rare-earth sublattice predominates at low temperatures; however, it decreases rapidly with the temperature and above $T_C = 246^\circ K$ (the compensation point) the magnetization of the total iron sublattice exceeds the magnetization of the sublattice of terbium ions.

The magnetic moment of the octahedral and tetrahedral sublattices of Fe^{3+} ions which are in the S state is a pure spin magnetic moment. The orbital moment of these ions in the cubic crystalline field is almost completely absent and the spin-orbit interaction is therefore small. In the case of the terbium ions the magnetic moment is produced by 4f electrons. The splitting due to the crystalline field are in this instance small, whereas the spin-orbit interaction is very large. The ground state of the Tb^{3+} ion is the 7F_6 state. The presence of an uncompensated orbital moment leads to large values of the crystallographic magnetic anisotropy energy and of the magneto-elastic energy of TbIG, especially at low temperatures.^[10,11]

4. MICROSCOPIC MECHANISMS OF THE MAGNETO-OPTIC EFFECTS IN RARE-EARTH IRON GARNETS

Let us consider the possible mechanisms of the magneto-optic effects within the framework of the polarizability tensor $\alpha_{ik}(\omega)$. For simplicity we shall assume that at optical frequencies the contribution of magnetic dipole transitions can be neglected.^[12,13] In those regions of the spectrum in which the magnetic permeability μ_{ik} differs from unity it is of course necessary to take also into account magnetic dipole transitions.

The contribution to the polarizability which depends on the magnetic moments \mathbf{M}^μ of the ions can be represented in the form of an expansion

$$\alpha_{ik}(\omega) = \sum_{\mu} A_{ikl}^{(\mu)}(\omega) M^{\mu} + \sum_{\mu} B_{iklm}^{(\mu)}(\omega) M^{\mu} M^m + \dots \quad (2)$$

where μ denotes the garnet sublattices and the indices i, k , and l denote the coordinates x, y , and z . In the absence of absorption the third-rank tensor $A_{ikl}(\omega)$ is antisymmetric with respect to transposition of indices.

As a result of summing over μ we obtain the polarizability of the elementary magnetic unit cell of the crystal. The contribution to $\mu_{ik}(\omega)$ linear in the magnetization components describes linear magneto-optic effects, for example the Faraday effect. We note that the frequency dependence of the tensor $A_{ikl}(\omega)$ should be different for nonequivalent sublattices and the FE can be observed even when the magnetic moments are compensating, for instance at the magnetic compensation point.

The magnitude of the FE is determined by the third order of perturbation theory,^[14] namely by taking into account twice the interaction of the electrons with the electric field of the light and by taking into account the

spin-orbit interaction. The anisotropy of the spin-orbit coupling of a single ion should lead to anisotropy of the FE in crystals. This anisotropy may turn out to be considerable in the case of the rare-earth iron garnets.^[15, 16]

The contribution to α_{ik} quadratic in the spin components describes the quadratic magneto-optic effects, for example the CME, and is determined by the following with respect to the FE order of perturbation theory with the spin-orbit interaction taken into account twice. The contribution is apparently small for 3d ions, but can turn out to be large for 4f ions for which the spin-orbit interaction is considerable. The contribution leads to the anisotropic CME.

As was shown in^[1], the cited expansion (2) is insufficient for describing magneto-optic effects in ferro- and antiferromagnets and one must take into account the polarizability due to the exchange interaction between different paramagnetic ions. This contribution to the polarizability written down in general form by Moriya^[14] in considering scattering in magnetic crystals, can also be used in the case of magneto-optic effects:

$$\alpha_{ik}^{\mu\nu}(\omega) = P_{ik}^{\mu\nu}(\omega)(\mathbf{M}^\mu \mathbf{M}^\nu) + \sum_{l,m} Q_{iklm}^{\mu\nu}(\omega) M_l^\mu M_m^\nu + \sum_{l,m} R_{iklm}^{\mu\nu}(\omega) M_l^\mu M_m^\nu + \dots, \quad (3)$$

where P_{ik} is a symmetric tensor, and Q_{iklm} and R_{iklm} are symmetric and antisymmetric tensors with respect to transposition of two magnetic moments.

The first term in (3), connected with the isotropic exchange interaction, makes a contribution to the polarizability in the third order of perturbation theory with twofold account of the electron-photon interaction and interion exchange. The second term in (3) appears only in the following order of perturbation theory and its contribution to the magneto-optic effects is obviously insignificant. The third term in (3) makes a contribution when account is taken of the exchange interaction and of the spin-orbit interaction, i.e., it is connected with anisotropic exchange.

Let us still dwell on one mechanism which can lead to a change in the phase velocities of light in a magnetically ordered crystal. As is known,^[10, 11] because of their large magnetostriction the rare-earth iron garnets are characterized by a strong increase of the magneto-elastic energy when the temperature is decreased. We shall write the change in the polarizability of a crystal under the action of elastic stresses in the form

$$\alpha_{ik}(\omega) = \hat{d}_{iklm}(\omega) U_{lm}, \quad (4)$$

where U_{lm} is a component of the deformation tensor and \hat{d}_{iklm} is the piezo-optic tensor symmetric with respect to pairs of indices i, k and l, m . For a cubic crystal the components of the deformation tensor can be expressed in terms of the magnetostriction constants λ_{100} and λ_{111} :

$$U_{ii} = 3/2 \lambda_{100} (\gamma_l^2 - 1/3)$$

and

$$U_{lm} = 3/2 \lambda_{111} \gamma_l \gamma_m, \quad (5)$$

where $\gamma_{l,m}$ are the direction cosines of the magnetization. Apparently, the components of the piezo-optic ten-

sor in magnetically ordered crystals are of the same order as in common materials, whereas in ferro- and antiferromagnets the magnetostriction constants are large. Thus for TbIG at 4.2°K $\lambda_{111} = 2420 \times 10^{-6}$ and $\lambda_{100} = 1200 \times 10^{-6}$.^[11] Such a large magnetostriction can lead to a considerable change in the symmetric components of the tensor α_{ik} , i.e., to an additional change of the phase velocity of the light waves in a magnetized crystal.

Let us note that since the tensors U_{lm} and \hat{d}_{iklm} in (4) are symmetric, magneto-elastic stresses can lead to linear birefringence of light but cannot make any contribution to the antisymmetric part of the tensor α_{ik} , i.e., cannot affect the magnitude of the FE directly. However, large magneto-elastic stresses can change the components of the tensor A_{ikl} in (2) and can in the final analysis change the magnitude of the antisymmetric components.

5. TEMPERATURE DEPENDENCE OF THE MAGNETIC BIREFRINGENCE

The temperature dependence of the magnetic birefringence when the external magnetic field is directed along the [100] and [111] directions is presented in Fig. 2. Even at room temperature one observes an anisotropy of the effect $\sim 3 \times 10^{-5}$ which reaches at 77°K a magnitude of 145×10^{-5} . At 77°K $\Delta n^{[100]}$ and $\Delta n^{[111]}$ have different signs. Since TbIG has an unusually high magnetostriction, we shall assume that the observed magnetic birefringence is due to the CME and to the magnetostriction:

$$\Delta n^{[100]} = \Delta n_{C-M}^{[100]} + \Delta n_{ms}^{[100]}, \quad (6)$$

and analogously for the [111] direction. The mechanisms leading to the anisotropy of Δn_{C-M} have been considered in Sec. 4, and the anisotropy of Δn_{ms} is connected with the anisotropy of the magnetostriction of TbIG.

A consideration of the $\Delta n(T)$ curves shows that the observed birefringence is related both to the CME and to the magnetostriction. In fact, at low temperatures the magnetostriction constants λ_{111} and λ_{100} have the same sign and the same type of temperature dependence, whereas $\Delta n^{[111]}$ and $\Delta n^{[100]}$ have different signs and opposite temperature dependences. In addition, at $T = 160^\circ\text{K}$ the constant λ_{100} passes through zero and the magnetic birefringence at this temperature is due to the CME. The contribution of the magnetostriction to the magnetic birefringence is in turn seen on the $\Delta n^{[100]}(T)$ and $\Delta n^{[111]}(T)$ curves in the region of the compensation point where because of the difference in the magnetostriction constants the jump in the magnetic birefringence for the two directions is unequal (Figs. 2 and 6, see below).

Thus the magnetic birefringence in TbIG is produced by the CME and by the piezo-optic effect; one cannot, however, separate the quantitative contribution of each of these effects from the available data. Such a separation can obviously be effected after investigating the CME in other iron garnets and after carrying out piezo-optic measurements.

At room temperature the sign of the birefringence $\Delta n^{[100]}$ and $\Delta n^{[111]}$ in TbIG is opposite to the sign of the

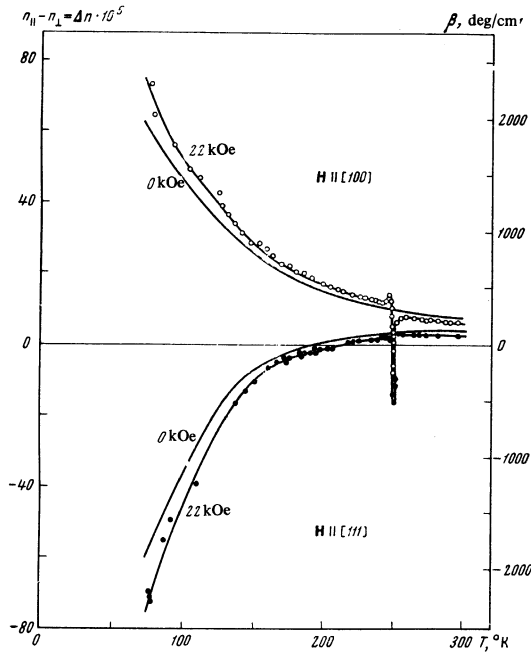


FIG. 2. Temperature dependence of the magnetic birefringence in TbIG. The magnitude is shown as the difference between the refractive indices (on the left) and as a phase difference (on the right). An external field of 22 kOe was applied along the [100] – light points, and along the [111] – black points. Solid curves – extrapolation to zero field.

CME in yttrium iron garnet (YIG).^[2] The different sign of the CME in TbIG and YIG attests to the fact that at this temperature the terbium sublattice and the total iron sublattice give an opposite sign of the effect and the CME of the terbium sublattice exceeds the CME of the iron sublattices. One observes then in the external magnetic field a decrease in the absolute magnitude of the birefringence on account of the paraprocess for $T > T_C$:

$$\Delta n(H) = \Delta n(M_s) - \Delta n(\chi_{Tb}H) - \Delta n(\chi_{Fe}H) \quad (7)$$

and an increase of it for $T < T_C$:

$$\Delta n(H) = \Delta n(M_s) + \Delta n(\chi_{Tb}H) + \Delta n(\chi_{Fe}H). \quad (8)$$

This is illustrated by the field dependence of the birefringence in Figs. 3 and 4. It should be noted that a complete measurement of $\Delta n(T)$ and $\Delta n(H)$ in YIG and TbIG makes it possible in principle to determine the proportionality constants in (7) and (8) in analogy with what was done for the FE in^[17]. The $\Delta n(H)$ dependence at 77°K (Figs. 3 and 4) indicates that the domain orientation upon application of any external magnetic field along the "easy" direction [111] ceases in fields of ~1–2 kOe and for the "difficult direction" [100] at ~4–5 kOe. Measurement of the birefringence allows one to follow the orientation of the magnetic moments in low fields.

Results for the case when $H \parallel [100]$ are presented in Fig. 5. In the absence of an external field the magnetic moments of the ions (M_S) are located along the [111] directions and their projections OA on the [110] perpendicular to the light ray, determine two values of Δn . The projection OB coincides with the light direc-

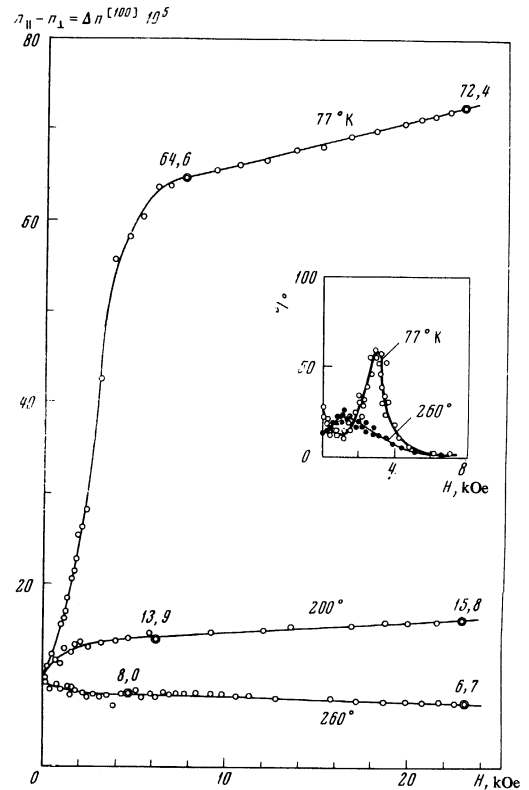


FIG. 3. Dependence of the magnetic birefringence on the external magnetic field $H \parallel [100]$ for 260° ($T > T_C$) and 200° and 77°K ($T < T_C$). The insert shows the percentage of depolarization of light transmitted through the crystal.

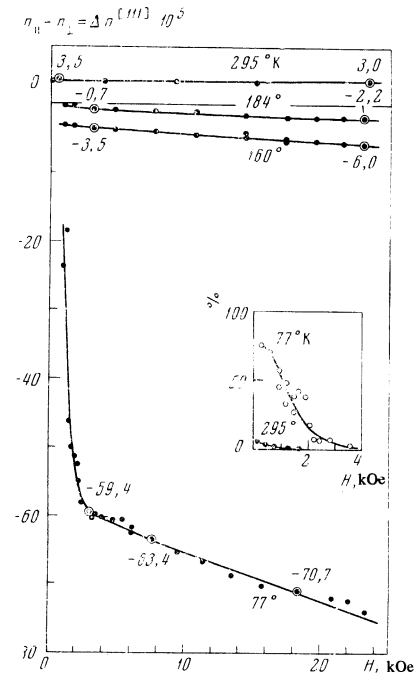


FIG. 4. Dependence of the magnetic birefringence on the external magnetic field $H \parallel [111]$ for 295° ($T > T_C$) and 184°, 160° and 77°K ($T < T_C$). The insert shows the percentage depolarization of light transmitted through the crystal.

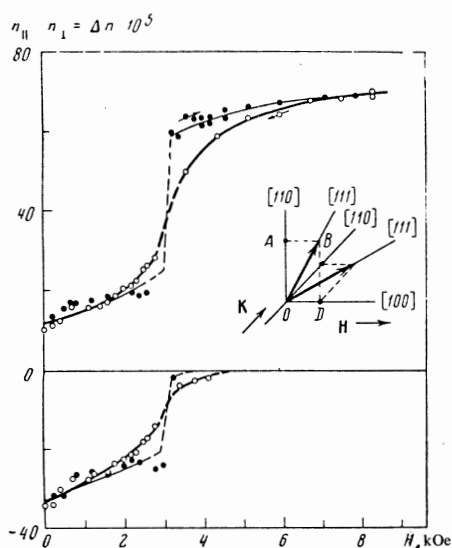


FIG. 5. Magnetic birefringence as a function of the external magnetic field applied along the [100] at 77°K. For $H = 0$ the effect is related to the projection of the spontaneous magnetization AO on the [110] (bottom) and $2 \times OD$ on the [100] (top). The diagram represents one of the octants of the investigated crystal containing $(2/8)M_S$ (black arrows).

tion \mathbf{k} and cannot therefore lead to birefringence (diagram in Fig. 5).

The process of orientation of the magnetic moments of the ions in an external field is accompanied by an increase in the depolarization of the light which reaches a maximum in a field of ~ 3 kOe (insert in Fig. 3). In this field there occurs a sharp increase of the birefringence connected with the projection of M_S on the [100] and a decrease of the birefringence determined by the projection of M_S on the [110]. Measuring the birefringence in a field applied along the [111], one can, of course, observe a similar situation. Depolarization of the light is also observed, albeit in a lower field (insert in Fig. 4). Analogous processes occur at higher temperatures, but the depolarization of the light is smaller and takes place in lower fields (inserts in Figs. 3 and 4).

6. OPTICAL PHENOMENA AT THE MAGNETIC COMPENSATION POINT

An anomaly of the quantities $\Delta n^{[111]}$ and $\Delta n^{[100]}$ was observed at the magnetic compensation point $T_C = 249^\circ\text{K}$ (Fig. 6). Such an anomaly was only determined in sufficiently high external magnetic fields; the anomaly was not observed for $H < 6$ kOe. Below and above T_C the Fe^{3+} and Tb^{3+} sublattices are oriented along the external magnetic field, however at the point T_C when the magnetic moments of the terbium and iron sublattices become equal, the crystal should behave magnetically like a compensated antiferromagnet placed in an external field. On approaching the compensation point, the magnetizations of the sublattices are directed along the external field and if we neglect the anisotropy in the plane perpendicular to \mathbf{H} (Fig. 7, a and b), then when the condition

$$H_{\text{ext}} > \sqrt{2H_a H_e} \quad (9)$$

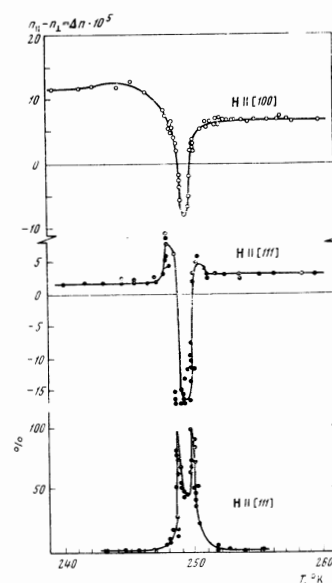
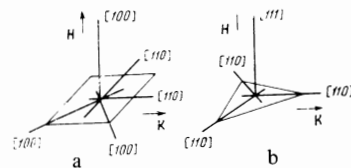


FIG. 6. Anomalies of the magnetic birefringence in the region of T_C in a field of 22 kOe applied along the [100] (top) and along the [111] (middle curve). At the bottom we present the depolarization of the light observed with $H = 22$ kOe applied along the [111].

FIG. 7. Diagram of the crystallographic directions for the garnet structure which lie in a plane perpendicular to the external magnetic field when the latter is applied along the [100] (a) and along the [111] (b).



is fulfilled, one should, as in the case of a uniaxial antiferromagnet, observe an inversion of the magnetic moments of the sublattices. For an anisotropy field $H_a \sim 10^3$ Oe and an exchange field $H_e \sim 10^5$ Oe the inversion occurs in fields $H_{\text{ext}} \sim 10^4$ Oe. This value agrees with the values of the inversion field (H_{inv}) obtained when investigating the FE in the vicinity of T_C .

The observed change of sign of the CME attests to the fact that at T_C there occurs in fact an inversion of the magnetic sublattices, since a change in the sign of the CME is equivalent to a change of the direction of magnetization by 90° . The inverted sublattices should of course orient themselves along the [110] axis—the direction of intermediate magnetization both in the case $H_{\text{ext}} \parallel [100]$ (Fig. 7a) as well as in the case $H_{\text{ext}} \parallel [111]$ (Fig. 7b). A part of the magnetic moments at the compensation point is thus oriented along the direction of the light (FE geometry) and a part of the magnetic moments is perpendicular to the direction of the light and leads to the existence of the CME at the magnetic compensation point.

On approaching T_C we observed an increase of the depolarization of the light at the crystal exit (lower curve in Fig. 6). The depolarization is caused by the fact that on approaching T_C in an external magnetic field the magnetic moments begin to deviate appreciably from the field direction and different parts of the crystal interact differently with the light. The deviation of the magnetic moments from the field direction leads to the situation in which composition of waves with a broad set of phases occurs at the crystal exit and one cannot achieve equalization of the phase differences with the aid of the compensator. The points of maximum de-

compensation coincide with the vanishing of magnetic birefringence on the $\Delta n(T)$ curves.

In the immediate proximity of the compensation point in the range $|T - T_C| \approx 0.5^\circ\text{K}$ the crystal exhibits in the presence of an external field antiferromagnetic properties—the moments of the sublattices are preferentially oriented perpendicular to the field. In this region one observes a decrease of the depolarization, which attests to a decrease in the spatial misorientation of the magnetic moments.

If T_C is passed in zero field or in low magnetic fields $H < H_{inv}$, then one should apparently not observe in the region of T_C any sharp change in the magnetic properties, say the susceptibility, of the crystal. However, on changing the temperature in sufficiently high magnetic field a transition should occur from the ferromagnetic to the antiferromagnetic phase followed by a second ferromagnetic phase:

$$\Phi_1 \rightarrow A\Phi \rightarrow \Phi_2.$$

The ferromagnetic phases 1 and 2 differ from one another in the magnitude of their magnetization in an external field. If below T_C

$$M_1 = M_s(T) + (\chi_{Tb} - \chi_{Fe})H, \quad (10)$$

where $M_s(T)$ is the spontaneous magnetization and χ is the sublattice susceptibility, and above T_C

$$M_2 = M_s(T) + (\chi_{Fe} - \chi_{Tb})H, \quad (11)$$

then the magnetization jump $\Delta M = M_1 - M_2$ in the region of T_C is

$$\Delta M \approx 2(\chi_{Tb} - \chi_{Fe})H, \quad (12)$$

i.e., the magnetization jump in the region of T_C is proportional to the external field.

Thus we have in the region of T_C in essence two phase transitions with both the $\Phi_1 \rightarrow A\Phi$ and $A\Phi \rightarrow \Phi_2$ transition being accompanied in an external field by a jump of the magnetization; in addition, $M_1 \neq M_2$.

An attempt was made to determine the light scattering which should accompany the magnetic phase transition. The conditions for setting up such an experiment were given in Sec. 2. In Fig. 8 we show the change of the light intensity reaching the photomultiplier cathode as a function of the temperature. It is seen that there are minima of the light intensity above and below T_C which are in good agreement with the maximum depolarization (Fig. 6). In this case too, as in the case of the CME and of the depolarization, the scattering was only observed in large magnetic fields.

Obviously, the observed scattering is related with the strong fluctuations of the magnetic moment in the region of T_C , and not with the domain structure which is, of course, absent in a field of 22 kOe.

The authors express their gratitude to M. F. Bryzhina and N. N. Syrnikova for orienting the crystal and to V. L. Ivanshintsova for help in carrying out the measurements.

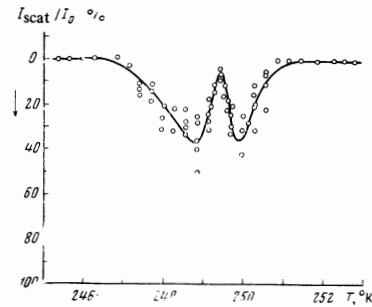


FIG. 8. Scattering of light in TbIG in the region of T_C .

¹ R. V. Pisarev, I. G. Siny, and G. A. Smolensky, *Sov. State Comm.* **7**, 23 (1969).

² R. V. Pisarev, I. G. Siniĭ, and G. A. Smolenskii, *ZhETF Pis. Red.* **9**, 112, 294 (1969) [*JETP Lett.* **9**, 64, 172 (1969)].

³ I. G. Siniĭ, R. V. Pisarev, P. P. Syrnikov, G. A. Smolenskii, and I. A. Kapustin, *Fiz. Tverd. Tela* **10**, 2252 (1968) [*Sov. Phys.-Solid State* **10**, 1775 (1969)].

⁴ F. S. Chen, H. J. Guggenheim, H. J. Levinstein, and S. Singh, *Phys. Rev. Lett.* **19**, 948 (1967).

⁵ J. C. Suits, B. E. Argyle, and M. F. Freiser, *J. Appl. Phys.* **37**, 1391 (1966).

⁶ V. B. Tatarskii, *Kristallogoptika i immersionnyĭ metod (Crystal Optics and the Immersion Method)*, Nedra, 1965.

⁷ F. Bertaut and F. Forrat, *Compt. Rend.* **242**, 382 (1956).

⁸ R. Pauthenet, *Ann. Phys.* **3**, 428 (1958).

⁹ S. Geller, J. P. Remeika, R. C. Sherwood, H. J. Williams, and J. P. Espinosa, *Phys. Rev.* **137**, A1034 (1965).

¹⁰ S. Iida, *J. Phys. Soc. Japan* **22**, 1201 (1967).

¹¹ V. I. Sokolov and Than Duc Hien, *Zh. Eksp. Teor. Fiz.* **52**, 1485 (1967) [*Sov. Phys.-JETP* **25**, 986 (1967)].

¹² L. D. Landau and E. M. Lifshitz, *Élektrodinamika sploshnykh sred (Electrodynamics of Continuous Media)*, Gostekhizdat, 1957.

¹³ P. S. Pershan, *J. Appl. Phys.* **38**, 1482 (1967).

¹⁴ T. Moriya, *J. Phys. Soc. Japan* **23**, 490 (1968).

¹⁵ V. M. Chetkin and A. N. Shalygin, *ZhETF Pis. Red.* **8**, 252 (1968) [*JETP Lett.* **8**, 154 (1968)].

¹⁶ G. S. Krinchik, *ZhETF Pis. Red.* **8**, 462 (1968) [*JETP Lett.* **8**, 284 (1968)].

¹⁷ R. W. Cooper, W. A. Crossley, J. L. Page, and R. F. Pearson, *J. Appl. Phys.* **39**, 565 (1968).

¹⁸ N. V. Kharchenko, V. V. Eremenko, and L. I. Belyi, *Zh. Eksp. Teor. Fiz.* **55**, 419 (1968) [*Sov. Phys.-JETP* **28**, 219 (1969)].